



# UNIVERSITÀ DI PARMA

## ARCHIVIO DELLA RICERCA

University of Parma Research Repository

Cyclosporine-loaded micelles for ocular delivery: Investigating the penetration mechanisms

This is the peer reviewed version of the following article:

*Original*

Cyclosporine-loaded micelles for ocular delivery: Investigating the penetration mechanisms / Ghezzi, Martina; Ferraboschi, Ilaria; Delledonne, Andrea; Pescina, Silvia; Padula, Cristina; Santi, Patrizia; Sissa, Cristina; Terenziani, Francesca; Nicoli, Sara. - In: JOURNAL OF CONTROLLED RELEASE. - ISSN 1873-4995. - 349:(2022), pp. 744-755. [10.1016/j.jconrel.2022.07.019]

*Availability:*

This version is available at: 11381/2932464 since: 2024-12-12T15:37:08Z

*Publisher:*

*Published*

DOI:10.1016/j.jconrel.2022.07.019

*Terms of use:*

Anyone can freely access the full text of works made available as "Open Access". Works made available

*Publisher copyright*

note finali coverpage

(Article begins on next page)

02 May 2026

1 **Cyclosporine-loaded micelles for ocular delivery: investigating the penetration mechanisms**

2

3 Martina Ghezzi<sup>1</sup>, Ilaria Ferraboschi<sup>2</sup>, Andrea Delledonne<sup>2</sup>, Silvia Pescina<sup>1</sup>, Cristina Padula<sup>1</sup>, Patrizia  
4 Santi<sup>1</sup>, Cristina Sissa<sup>2</sup>, Francesca Terenziani<sup>2</sup>, Sara Nicoli<sup>1\*</sup>

5

6 <sup>1</sup> ADDRes Lab, Department of Food and Drug, University of Parma, Parco Area delle Scienze 27/A,  
7 43124 Parma, Italy

8

9 <sup>2</sup> Department of Chemistry, Life Science and Environmental Sustainability, University of Parma,  
10 Parco Area delle Scienze 17/A, 43124 Parma, Italy

11

12

13 \*Corresponding Author:

14

15 Sara Nicoli PhD

16 ADDRes Lab (Advanced Drug Delivery Research Lab)

17 Department of Food and Drug

18 University of Parma

19 Parco Area delle Scienze, 27/A

20 43124 Parma, Italy

21 Telefono +39 0521 905065/71

22 Fax +39 0521 905006

23 E-mail: [sara.nicoli@unipr.it](mailto:sara.nicoli@unipr.it)

24

25

26 Submitted to: Journal of Controlled Release

27

28

29

30 Abstract:

31 Cyclosporine is an immunomodulatory drug commonly used for the treatment of mild-to-severe dry  
32 eye syndrome as well as intermediate and posterior segment diseases as uveitis. The ocular  
33 administration is however hampered by its relatively high molecular weight and poor permeability  
34 across biological barriers. The aim of this work was to identify a micellar formulation with the ability  
35 to solubilize a considerable amount of cyclosporine and promote its transport across ocular barriers.

36 Non-ionic amphiphilic polymers used for micelles preparation were tocopherol polyethylene glycol  
37 1000 succinate (TPGS) and Solutol® HS15. Furthermore, the addition of alpha-linolenic acid was  
38 assessed. A second aim was to evaluate micelles fate in the ocular tissues (cornea and sclera) to  
39 shed light on penetration mechanisms. This was possible by extracting and quantifying both drug  
40 and polymer in the tissues, by studying TPGS hydrolysis in a bio-relevant environment and by  
41 following micelles penetration with two-photon microscopy. Furthermore, TPGS role as permeation  
42 enhancer on the cornea, with possible irreversible modifications of tissue permeability, was  
43 analyzed. Results showed that TPGS micelles (approx. 13 nm in size), loaded with 5 mg/ml of  
44 cyclosporine, promoted drug retention in both the cornea and the sclera. Data demonstrated that  
45 micelles behavior strictly depends on the tissue: micelles disruption occurs in contact with the  
46 cornea, while intact micelles diffuse in the interfibrillar pores of the sclera and form a reservoir that  
can sustain over time drug delivery to the deeper tissues. Finally, cornea quickly restore the barrier

47 properties after TPGS removal from the tissue, demonstrating its potential good tolerability for  
48 ocular application.

49

50 Keywords: cyclosporine, polymeric micelles, corneal delivery, transscleral delivery, TPGS hydrolysis,  
51 two-photon microscopy

52

53 Highlights

54 • TPGS micelles improved cyclosporine solubility promoting its retention in eye tissues

55 • Micelles disassemble in contact with the cornea

56 • Micelles diffuse intact inside the scleral tissue

57 • TPGS is hydrolyzed by tissue esterases when in contact with cornea and sclera

58 • Two-photon microscopy is a useful tool to study micelles-tissues interaction

59

60

61 **1. Introduction**

62 Cyclosporine A (CYC), a neutral cyclic peptide isolated from different fungal species, is an  
63 immunomodulatory drug which works inhibiting T cells activation by blocking the transcription of  
64 cytokine genes including those encoding for IL-2 and IL-4 [1]. Its main ocular application is the  
65 treatment of mild-to-severe dry eye syndrome (DES) and, with this indication, it is present as anionic  
66 O/W emulsion on the US market (0.05%, Restasis®) and as a cationic O/W nanoemulsion (0.1%,  
67 Ikervis®) on EU market. Moreover, an ophthalmic solution (0.09%, Cequa®) has been recently  
68 approved by the Food and Drug Administration. Together with the treatment of DES and other  
69 corneal affections [2, 3], cyclosporine has demonstrated its activity for the treatment of blepharitis  
70 [4, 5] as well as intermediate and posterior segment diseases including uveitis [6, 7] and Behçet  
71 disease [8].

72 The formulation of this drug and its delivery to ocular tissues are however hampered by its relatively  
73 high molecular weight (1202.6 g/mol), poor water solubility [9] and marked lipophilicity (log P= 3  
74 [10]). Therefore, cyclosporine A is mainly administered via oily and surfactant-containing  
75 formulations [11], presenting low tolerability and side effects, such as ocular burning, vision  
76 interference, eye irritation and conjunctival hyperaemia [9, 12]. Moreover, cyclosporine higher  
77 affinity for the oily phase rather than the aqueous environment usually results in a poor  
78 bioavailability [12]. A possible alternative to solve these issues is represented by the use of micelles,  
79 i.e. colloidal systems formed by self-assembling of amphiphilic molecules ~~polymers~~ in solution at a  
80 concentration above the Critical Micellar Concentration (CMC). Surfactant micelles, made by low  
81 molecular weight compounds, show high CMC and thus low physical stability. On the contrary,  
82 polymeric micelles, i.e. micelles formed by amphiphilic polymers, are characterized by lower CMC  
83 and better stability against dilution, and are generally preferred as drug delivery systems. Micelles  
84 are composed of an inner lipophilic core, involved in drug loading and release, and an external  
85 hydrophilic shell, responsible for micelles interaction with body targets. These nanosystems, in  
86 addition to a relatively easy preparation, sterilization method and high scale-up feasibility, showed  
87 good solubilization properties and efficient cellular internalization [13-15]. In case of ocular delivery,  
88 micelles have demonstrated the ability to enhance drug transport to the anterior eye segment [16-  
89 18] thanks to an improved solubility of drugs, higher penetration capacity (due to their nanometric  
90 size) and prolonged drug release [19-21]. Furthermore, ex-vivo data highlighted their capability to  
91 promote drug permeation across ocular tissues such as the sclera and the choroid, in the perspective  
92 of a posterior segment targeting [16, 21, 22]. It is also worth mentioning that an extremely recent  
93 review identifies the word "micelles" as one of latest high-frequency keywords, including this  
94 vehicle among the emerging frontiers in ocular drug delivery [23]. Unfortunately, the intense  
95 academic research has not necessarily been followed by actual industrial development. The reasons  
96 are different, related to stability problems and difficulty of characterization [13, 24], but also to the  
97 scarce information available regarding the fate of the polymer following ocular administration. This  
98 aspect should be investigated since it provides numerous information: first of all, the quantification  
99 of the polymer in the various tissues allows us to elucidate the transport mechanisms, a non-trivial  
100 action in the case of micelles that, being association colloids, can undergo considerable and rapid  
101 changes following interaction with biological fluids and tissues. Alongside this aim, to follow the  
102 "destiny" of the polymer is extremely important under a toxicological point of view: this is

103 particularly relevant when the target is represented by the posterior segment of the eye, because  
104 in this case a contact between the polymer and the retina can be envisaged.

105

106 Thus, the idea behind this work was to identify a micellar formulation with the ability to solubilize a  
107 relevant amount of cyclosporine and promote its transport across ocular barriers. Non-ionic  
108 amphiphilic polymers used for micelles preparation were tocopherol polyethylene glycol 1000  
109 succinate (TPGS) and Solutol® HS15. Furthermore, the addition of alpha-linolenic acid was assessed,  
110 in the light of the interesting results reported on fatty acids for micelles preparation [25, 26] and  
111 increased drug loading [27, 28]. A second aim was to evaluate micelles fate in the ocular tissues  
112 (cornea and sclera) to shed light on the penetration mechanisms. This was possible by quantifying  
113 both drug and polymer in the tissues, by studying TPGS hydrolysis in a bio-relevant environment  
114 and by following micelles penetration with two-photon microscopy.

## 115 **2. Materials and methods**

116

### 117 **2.1. Materials**

118

119 Cyclosporine A (MW 1202.6 g/mol; logP 3; water solubility 27.67 µg/ml [29]) was purchased from  
120 Alfa Aesar (Kandel, Germany) while tocopheryl polyethylene glycol 1000 succinate (TPGS) was  
121 received from PMC ISOCHEM (Vert-Le-Petit, France). Alpha-linolenic acid (LA; MW 278.43 g/mol;  
122 logP 6.46; pK<sub>a</sub> 4.77), fluorescein sodium (MW 376.28 g/mol) and Nile red (NR; 9-(diethylamino)-5H-  
123 benzo[a]phenoxazin-5-one; MW 318.4 g/mol) were purchased from Sigma-Aldrich (Saint Louis, MO,  
124 USA). Solutol® HS15 was received from BASF (Ludwigshafen, Germany) whereas citric acid and  
125 propylene glycol were purchased from A.C.E.F. S.p.a (Fiorenzuola d'Arda, Italy). For HPLC analysis  
126 high purity water (Purelab® Pulse, Elga Veolia,UK) and HPLC grade acetonitrile were used. Acetate  
127 buffer was prepared by mixing 0.1 M acetic acid and 0.1 M sodium acetate solutions in 82:18 (v/v)  
128 ratio; pH was adjusted to 4.8 using 0.1 M NaOH. Simulated tear fluid (STF) was obtained by  
129 solubilizing in water CaCl<sub>2</sub> 0.06 g/l, NaHCO<sub>3</sub> 2.18 g/l and NaCl 6.7 g/l; pH was adjusted to 7.4 using  
130 1M HCl. Phosphate Buffer Saline (PBS) was prepared by dissolving in high purity water KH<sub>2</sub>PO<sub>4</sub> 0.19  
131 g/l, Na<sub>2</sub>HPO<sub>4</sub> 2.37 g/l and NaCl 8.8 g/l; pH was adjusted to 7.4 using H<sub>3</sub>PO<sub>4</sub> 85%. HEPES buffer was  
132 prepared by solubilizing in high purity water HEPES 5.96 g/l and NaCl 9 g/l; pH was adjusted to 7.4  
133 using NaOH 5M.

134

### 135 **2.2. Cyclosporine and linolenic acid quantification method**

136

137 Cyclosporine and linolenic acid quantification was performed using an HPLC-UV system (Infinity  
138 1260, Agilent Technologies, Santa Clara, CA, USA), with a reverse-phase column (Aeris™ WIDEPOR  
139 XB-C<sub>8</sub> column, 150 x 4,60 mm, 3,6 µm, Phenomenex, Torrance, CA, USA) thermostated at 65°C. The  
140 mobile phase was composed of CH<sub>3</sub>CN:water with TFA 0.1% in ratio 55:45 (v/v). The flow was  
141 maintained at 1.6 ml/min and the injection volume was equal to 100 µl. The retention time of  
142 cyclosporine and linolenic acid, both quantified by UV absorbance at 230 nm, was respectively of  
143 4.9 and 3.1 minutes. For cyclosporine, linearity was found in the interval 1-50 µg/ml, whereas for

144 linolenic acid in the range 5-100 µg/ml. Details on calibration curves, RSD%, RE% and LOQ values, as  
 145 well as discussion on the method and the impact of the injection solvent are reported in the  
 146 supplementary materials (see par. 1.1).

147

### 148 2.3. TPGS quantification method

149

150 TPGS quantification, performed with a previously validated method [30], was done using an HPLC-  
 151 UV system (Infinity 1260, Agilent Technologies, Santa Clara, CA, USA), with a reverse-phase C18  
 152 column (Waters, Symmetry300 C18, 5 µm, 4.6 × 250 mm) and a C18 guard column (SecurityGuard  
 153 Widepore C18, Phenomenex, Torrance, CA, USA), thermostated at 40 °C. The mobile phase,  
 154 composed of acetate buffer pH 4.8:CH<sub>3</sub>OH in 3:97 (v:v) ratio, was pumped at 2 ml/min. The retention  
 155 time of TPGS, quantified by UV absorbance at 215 nm, was 4 minutes while the injection volume  
 156 was 100 µl. Calibration curves were built in the concentration interval 1-25 µg/ml. Samples were  
 157 injected without previous dilution. Further information on the preparation of the standards for the  
 158 calibration curve are reported in the supplementary materials (see par. 1.2).

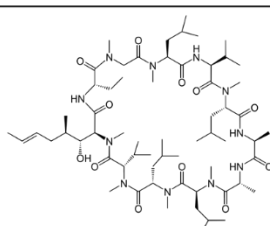
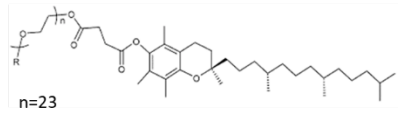
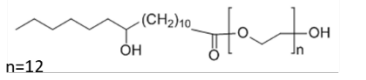
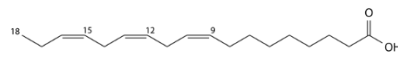
159

### 160 2.4. Preparation of blank polymeric micelles

161 Polymeric micelles were prepared by direct dissolution of TPGS and/or Solutol® HS15 in high purity  
 162 water to obtain formulations S (Solutol®), ST (Solutol® and TPGS) and T (TPGS) (see Figure 1 for  
 163 details on the structure and table 1 for details on the composition of micellar formulations).

164

165 Figure 1: Drug and excipients used for micelles preparation with their main chemical features and molecular structure.

Compound	Molecular weight (g/mol)	Log P	HLB	pK <sub>a</sub>	H-bond capacity (donor-acceptor)	Molecular structure
Cyclosporine	1202.6	2.92	-	13.3	5-12	
TPGS	1513	-	13.2	-	1-6	
Solutol® HS15	963.2	-	14-16	-	3-19	
Linolenic acid	278.4	6.46	-	4.77	1-2	

166

167

168 8 ml of S, ST and T micelles were then added with 100 µl of linolenic acid (L) this becoming SL, STL,  
 169 TL, respectively, and vortexed (3 times x 20 sec each) in order to ensure complete saturation of the  
 170 aqueous phase. Afterwards, to separate linoleic acid and obtain a clear solution, the oily phase was  
 171 removed by 2-folds filtration (regenerated cellulose, Sartorius Minisart RC 0.2 µm). The amount of

172 linolenic acid loaded in the micelles was then evaluated by HPLC after proper dilution with the  
173 mobile phase.

174  
175 Table 1: Blank micellar formulations with relative composition and codification.

CODE	TPGS (mM)	SOLUTOL® HS15 (mM)	LINOLENIC ACID
T	20	-	-
S	-	20	-
ST	10	10	-
TL	20	-	at saturation
SL	-	20	at saturation
STL	10	10	at saturation

176

## 177 2.5. Cyclosporin-loaded polymeric micelles

178

179 In order to determine cyclosporine solubility, the blank micellar formulations (see table 1 for the  
180 compositions) were added with an excess of the drug, sonicated for 3 minutes and left under  
181 magnetic stirring at room temperature for at least 72 h. Then, the suspension was centrifuged at  
182 10,000 rpm for 15 minutes and, when needed, for other 20 minutes at 15,000 rpm to get complete  
183 precipitation of the undissolved drug and obtain a limpid formulation. The supernatant was sampled  
184 and analyzed by HPLC-UV for determining the solubility of both cyclosporine and linolenic acid after  
185 proper dilution with the mobile phase. Cyclosporine solubility is reported as mean  $\pm$  SD;  $n \geq 9$  for T  
186 micelles,  $n \geq 3$  for the other formulations.

187 Size and polydispersity index (PDI) of blank and CYC-loaded micelles were measured by Dynamic  
188 Light Scattering (DLS) using a Zetasizer Nano-ZSP (Malvern Instruments, Malvern, UK).  
189 Measurements were performed at 25 °C after 10-folds dilution in high purity water.

190

## 191 2.6. Tissue preparation

192

193 Fresh porcine eyes were isolated from Landrace and Large White (age 10–11 months, weight 145–  
194 190 kg), female and male animals supplied from a local slaughterhouse (Macello Annoni S.p.A.,  
195 Parma, Italy). The eyes were kept in PBS at 4 °C until the dissection, which occurred within 2 h from  
196 the enucleation. The muscular and connective tissues around the eye bulb were completely  
197 removed. For corneal permeation experiments, only bulbs with macroscopically intact corneas were  
198 used, whereas eyes showing opaque corneas were discarded. The cornea, isolated as a corneo-  
199 scleral button-shaped piece, was obtained cutting with a scalp beyond the limbus. For scleral  
200 permeation, the isolated sclera was obtained by circumferentially cutting and removal of the  
201 anterior segment of the eye behind the limbus. The collected eyecup was then cut and everted. The  
202 neural retina and the choroid-Bruch's layer were discarded while the sclera was used for the  
203 permeation experiment.

204

## 205 2.7. Study of the effect of TPGS on cornea permeability: transcorneal permeation of 206 fluorescein

207

208 In order to evaluate if TPGS induces an increase of corneal permeability, the permeation of sodium  
209 fluorescein was evaluated after application of TPGS micelles to the tissue for 10 minutes. The tissue  
210 was mounted on a glass Franz-type vertical diffusion cell (DISA, Milano, Italy) with a permeation  
211 area of 0.2 cm<sup>2</sup>. The receptor was filled with HEPES buffer pH 7.4 (about 4 ml, exactly measured)  
212 magnetically stirred at 37°C to guarantee sink conditions. First, the donor was pre-treated with 200  
213 µl of TPGS 20 mM micelles for 10 min. Afterwards, the formulation was removed and the tissue was  
214 washed 3 times with 200 µl of HEPES buffer and carefully dried with a cotton swab. A solution of  
215 fluorescein sodium (1.18 mg/ml) was then applied at infinite dose (200 µl/cm<sup>2</sup>) for 4 h. 300 µl of  
216 receptor solution were sampled at different timepoints (0, 1, 1.5, 2, 3 and 4 hours from the  
217 deposition of the formulation) and the receptor was filled with fresh HEPES buffer. Negative and  
218 positive controls were also evaluated. The negative control was represented by a pre-treatment of  
219 10 minutes with HEPES buffer (pH 7.4). The positive control was represented by a 0.1% p/v  
220 benzalkonium chloride solution applied for 5 or 10 minutes.  
221 The samples fluorescence ( $\lambda_{exc}=490$  nm,  $\lambda_{em}=535$  nm) was measured via microplate reader (SPARK10  
222 M, TECAN, Mannendorf, CH). More information on the preparation of the calibration curve, RSD%,  
223 RE% and LOQ values are reported in the supplementary materials (par. 1.3). All experiments were  
224 carried out using different ocular bulbs from different animals. The amount of fluorescein sodium  
225 permeated (µg/cm<sup>2</sup>) was reported as a function of time (min). The transcorneal flux across the  
226 cornea (J, µg/cm<sup>2</sup>h) was determined as the slope of the regression line at the steady state, while the  
227 apparent permeability coefficient (P, cm/s) was calculated at the steady state as:  $P=J/C_d$ , where  $C_d$   
228 (µg/ml) is the concentration of the donor solution. Data are reported as mean ± SD; number of  
229 replicates was  $n \geq 3$ , unless differently indicated.

## 231 **2.8. Retention and permeation experiments across cornea and sclera**

232  
233 The tissue was mounted on a glass Franz-type vertical diffusion cell (DISA, Milano, Italy) with a  
234 permeation area of 0.2 cm<sup>2</sup> (cornea) or 0.6 cm<sup>2</sup> (sclera). The set-up used for corneal permeation  
235 experiments was previously validated to guarantee that tissue barrier properties were preserved  
236 throughout the experiment duration [31]. The receptor was filled with PBS pH 7.4 (4 ml, exactly  
237 measured) that was magnetically stirred to guarantee sink conditions. The formulations were  
238 applied at infinite dose (200 µl/cm<sup>2</sup>, occluded). At the end of the experiment, the receptor solution  
239 was sampled, the formulation was removed from the donor and the tissue was rinsed 3 times with  
240 PBS. Therefore, cyclosporine and TPGS were extracted by treating tissues with 1 ml solution of  
241 CH<sub>3</sub>CN:CH<sub>3</sub>COOH 1% in 87:13 ratio. Samples were left under these conditions overnight at room  
242 temperature, then sonicated for 12 minutes and centrifuged at 12,000 rpm for 15 min before HPLC  
243 analysis. This extraction method, previously validated for cyclosporine [30], was also challenged for  
244 its ability to extract TPGS. The percentage of recovery found for TPGS was  $91.9 \pm 3.15$  %. In case of  
245 cornea, experiment duration was 5 h and CYC-loaded formulations tested were T, TL and ST (see the  
246 composition in Table 1 and CYC solubility in Figure 2). In case of sclera, only T was evaluated. The  
247 experiments were performed for 6 and 48 h. Additionally, to evaluate the reservoir effect of the  
248 tissue, T was applied to the sclera for 6 h; then, the formulation was carefully removed, the sclera  
249 surface was dried with a cotton bud and permeation experiment was continued up to 48 h. After

250 this time, cyclosporine was extracted from the sclera and quantified in the receptor phase, as  
251 previously described. Data are reported as mean  $\pm$  SD;  $n \geq 3$  for all formulations.

252

## 253 **2.9. Hydrolysis of TPGS in contact with ocular tissues**

254

255 The in vitro enzymatic hydrolysis of TPGS was evaluated using cornea and sclera excised from fresh  
256 porcine eyes. In particular, the isolated tissues were punch-biopsied with a 0.9 mm punch and cut  
257 in four pieces of the same size.

258 A solution of TPGS with concentration 100  $\mu\text{g}/\text{ml}$  was prepared by dissolving the polymer in a  
259 mixture of PBS pH 7.4:water in ratio 1:10. Then, 300  $\mu\text{l}$  of TPGS 100  $\mu\text{g}/\text{ml}$  were incubated with two  
260 pieces of the tissue (average weight 50 mg for cornea and 60 mg for sclera) for 24 h (for the cornea)  
261 and 48 h (for the sclera) at 37°C. At predetermined time intervals, samples were centrifuged at  
262 12,500 rpm for 5 minutes and 40  $\mu\text{l}$  of the TPGS solution were withdrawn and diluted 1:10 with  
263  $\text{CH}_3\text{CN}:\text{CH}_3\text{COOH}$  1% (87:13), causing esterase inactivation. The concentration of TPGS in these  
264 samples was measured by HPLC. Control samples obtained in the same conditions but without tissue  
265 were analyzed as well.

266

## 267 **2.10. Two-photon microscopy**

268

269 For the two-photon microscopy analysis, Nile red-loaded TPGS 20 mM micelles were prepared.  
270 Briefly, 10  $\mu\text{l}$  of a 10 mg/ml NR solution in DMSO were added to 1.5 ml of blank TPGS 20 mM  
271 micelles. The sample was then centrifuged at 13,000 rpm for 5 min to precipitate the exceeding NR  
272 and to collect the supernatant. Afterwards, the corneal or the scleral tissue was mounted on a Franz-  
273 type vertical diffuse cell (0.6  $\text{cm}^2$ ). The donor was filled with 120  $\mu\text{l}$  of NR-loaded TPGS micelles,  
274 while the receptor was filled with PBS pH 7.4 under magnetic stirring. The experiment duration was  
275 2 h. The same experiment was performed also using a reference NR saturated aqueous solution  
276 prepared by adding 10  $\mu\text{l}$  of a 10 mg/ml NR solution in DMSO to 1.5 ml of high purity water and  
277 centrifuging following the conditions previously reported to collect the supernatant.

278 Porcine samples were analyzed with a Two-Photon Microscope Nikon A1R MP+ Upright equipped  
279 with a femtosecond pulsed laser Coherent Chameleon Discovery ( $\sim 100$  fs pulse duration with 80  
280 MHz repetition rate, tunable excitation range 660-1320 nm). A 25 $\times$  water dipping objective with  
281 numerical aperture 1.1 and 2-mm working distance was employed for focusing the excitation beam  
282 and for collecting the two-photon excited fluorescence (TPEF) and the second harmonic generation  
283 (SHG) signals. TPEF/SHG signal was directed by a dichroic mirror to a series of three non-descanned  
284 detectors (high sensitivity GaAsP photomultiplier tubes) allowing fast image acquisition. The three  
285 detectors are preceded by optical filters allowing the simultaneous acquisition of three separated  
286 channels: blue channel (415–485 nm), green channel (506–593 nm) and red channel (604–679 nm).  
287 Imaging overlay of the three channels and processing was performed by the operation software of  
288 the microscope. Additionally, a fourth GaAsP photomultiplier detector, connected to the  
289 microscope through an optical fiber and preceded by a dispersive element, was used to record the  
290 spectral profile of the TPEF/SHG signal (wavelength range 430 to 650 nm with a bandpass of 10 nm).

291 For microscope observations, performed right after dismounting the tissue from the Franz-type cell,  
292 the samples were placed in a dedicated plexiglass holder and saline solution was used to dip the  
293 objective and to avoid dehydration. Two different excitation wavelengths were used, 860 or 1080  
294 nm. Images were acquired with a typical field of view of 500  $\mu\text{m}$   $\times$  500  $\mu\text{m}$ , except where explicitly  
295 reported.

296 Besides two-photon microscopy analysis, the emission spectrum of NR-loaded TPGS micelles and a  
297 NR solution in water were registered with an Edinburgh FLS-1000 fluorimeter. The solutions were  
298 prepared by adding 20  $\mu\text{L}$  of a 400  $\mu\text{M}$  DMSO NR stock solution in 3 mL of 0.5 mM TPGS micelles or  
299 high purity water (final NR concentration 2.7  $\mu\text{M}$ , total percentage of DMSO < 1%) which were then  
300 filtered after the preparation (hydrophilic PTFE, AISIM  $\hat{\text{O}}$  0.22  $\mu\text{m}$ ).

301

### 302 **2.11. Statistical analysis**

303 All data presented in text, figures and tables are reported as mean value  $\pm$  SD. The significance of  
304 the differences between the results was assessed using Student's t-test. Differences were  
305 considered statistically significant when  $p < 0.05$ .

306

## 307 **3. Results and discussion**

308

309 Polymeric micelles have demonstrated to be powerful tools to overcome the drawbacks of  
310 traditional ocular dosage forms, with particular potentialities for an improved drug administration  
311 to the anterior segment of the eye. Indeed, micelles can be used to formulate hydrophobic  
312 compounds as aqueous solutions which, applied as eye drops, can easily mix with the lacrimal fluid  
313 without causing any vision interference [14, 32].

314

### 315 **3.1. Cyclosporine solubility studies**

316

317 The first part of the work was dedicated to the identification of micellar formulas capable of  
318 increasing cyclosporine aqueous solubility, that is very low; in simulated tear fluid we found a  
319 solubility lower than 5  $\mu\text{g}/\text{ml}$ .

320 The polymers used were TPGS and Solutol<sup>®</sup> HS15, alone or combined in a 1:1 molar ratio. TPGS, was  
321 selected for the possible release of antioxidant vitamin E via enzymatic hydrolysis [30]. Moreover,  
322 this polymer previously demonstrated its permeation enhancing properties for several drugs  
323 through the corneal tissue [33-35] probably related also to P-glycoprotein inhibition [36]. Solutol<sup>®</sup>  
324 HS15 was selected considering its capacity to improve hydrophobic drugs solubility [37, 38] and its  
325 promising outcomes regarding the enhancement of corneal permeability and retention [39].  
326 Linolenic acid was also added to the micellar formulations (see table 1 for detailed composition and  
327 codification) since data previously collected in our laboratory demonstrated the capability of fatty  
328 acids to increase the encapsulation of an hydrophobic compound [27]. Additionally, linolenic acid is  
329 a precursor of prostaglandin E1, a potent anti-inflammatory agent capable of reducing the ocular  
330 inflammation [40], promoting tear production and decreasing DES symptoms [41]. Some studies  
331 demonstrated that dietary supplementation with linolenic acid led to a reduction of ocular surface

332 inflammation in patients with DES [42, 43] and there is also some evidence of omega-3 fatty acids  
333 effectiveness when applied topically [44, 45].

334

335 TPGS and Solutol® demonstrated a similar capability to dissolve linolenic acid (4 mg/ml). However,  
336 their 1:1 mixture reduced linolenic acid solubility by half. Cyclosporine was then added to the  
337 micelles; TPGS alone gave the highest cyclosporine solubility ( $5.26 \pm 0.39$  mg/ml) and Solutol® the  
338 lowest ( $0.57 \pm 0.1$  mg/ml). In the presence of linolenic acid, the solubility of cyclosporine decreased  
339 (Table 2) regardless the polymers composition. Also the concentration of linolenic acid after  
340 cyclosporine loading (Table 2) showed to be markedly reduced by cyclosporine presence; this  
341 suggests a competition between the two molecules for the interaction with the micellar core, whose  
342 size is relatively small [27]. This result differs from the previously published data on imiquimod,  
343 where fatty acids co-encapsulation was used to increase the solubility of this hydrophobic drug into  
344 TPGS micelles [27].

345

346 Table 2. Solubility of cyclosporine (CYC) and linolenic acid (LA) alone and combined in the micellar formulations.  
347 Formulations further evaluated are indicated in bold.

348

	FORMULATION	CYC SOLUBILITY (mg/ml)	LA SOLUBILITY (mg/ml)
<i>cyclosporine only</i>	T	$5.26 \pm 0.39$	-
	S	$0.57 \pm 0.1$	-
	ST	$3.27 \pm 0.28$	-
<i>linolenic acid only</i>	TL	-	$3.82 \pm 0.11$
	SL	-	$4.26 \pm 0.32$
	STL	-	$2.37 \pm 0.31$
<i>cyclosporine and linolenic acid</i>	TL	$3.04 \pm 0.52$	$0.60 \pm 0.03$
	SL	n.d.	n.d.
	STL	$0.53 \pm 0.09$	1.240.25

349

350 Given the results obtained, the formulations T, TL and ST loaded with cyclosporine were selected  
351 for further studies, since they guarantee a drug solubility equal or higher than 3 mg/ml and, in the  
352 case of TL, also the presence of linolenic acid that can support drug action. Additionally, these  
353 formulations were selected also for their stability, evaluated after approx. 2 months as reported in  
354 Figure S2.

355

356 The size of the drug-loaded micelles, reported in Table 3, is between 13 and 16 nm. Details on DLS  
357 analysis including data on discarded formulations and blank micelles are presented in  
358 supplementary material (Table S2). The size of TPGS as well as Solutol® micelles demonstrated to  
359 be in good agreement with values reported in the literature [46, 47] and minor changes in micelle  
360 size were reported after addition of linolenic acid or after cyclosporine loading, despite the increase  
361 in the polydispersity index.

362

363 **3.2. Cyclosporine and TPGS accumulation and retention in ocular tissues**

364 The role of the micellar formulation on drug delivery to the ocular structures has not been fully  
365 clarified. An increased solubility, the permeation enhancing properties of the polymer and the  
366 uptake of intact micelles seem to concur to the increased drug penetration [48], however, the  
367 contribution of each mechanism is difficult to deduce. In fact, given the nature of these nanocarriers,  
368 formed by an association of amphiphilic unimers, the study of the interaction with the biological  
369 environment is particularly hard. In this paper, to elucidate the micelles behaviour upon contact  
370 with the biological barriers, we quantified both drug and polymer (TPGS) inside the ocular  
371 structures.

372  
373 **3.2.1. Cyclosporine and TPGS retention into the cornea**

374 Formulations T, TL and ST loaded with CYC at saturation were then applied to the corneal tissue to  
375 evaluate their capability to promote drug uptake into the epithelial cells. At the end of the  
376 experiment, the drug was extracted from the tissue with a validated method [30]. This method was  
377 also challenged for its ability to extract TPGS that can likewise accumulate in the cornea. The results  
378 obtained in term of cyclosporine and TPGS accumulation from these formulations are presented in  
379 Table 3, while the amount of polymer and drug permeated is not reported as no transcorneal  
380 permeation occurred.

381  
382 Table 3. Composition, size and CYC solubility of the CYC-loaded micellar formulations evaluated on the corneal tissues.  
383 Data on drug and TPGS accumulation in the cornea are also reported.

Micelles characteristics				Cyclosporin and TPGS delivery to the cornea	
	Composition	Size (nm) ( <i>PDI</i> )	Cyclosporine conc. (mg/ml)	Cyclosporine in corneal tissue ( $\mu\text{g}/\text{cm}^2$ )	TPGS in corneal tissue ( $\mu\text{g}/\text{cm}^2$ )
T	TPGS 20 mM	$12.96 \pm 4.03^{[46]}$ (0.091)	$5.26 \pm 0.39$	$19.81 \pm 4.49$	$55.92 \pm 26.25$
TL	TPGS 20 mM saturated with linolenic acid	$14.47 \pm 4.91$ (0.196)	$3.04 \pm 0.52$ (linolenic acid: $0.60 \pm 0.03$ )	$2.82 \pm 1.43$	$41.05 \pm 22.92$
ST	TPGS 10 mM and Solutol® 10 mM	$15.65 \pm 5.90$ (0.213)	$3.27 \pm 0.28$	$2.35 \pm 0.66$	$2.82 \pm 0.08$

384  
385 Formulation T outperformed the others, with an amount of drug accumulated about 7-fold higher.  
386 Both the addition of linolenic acid (TL) or Solutol® (ST) decreased micelles delivery efficiency. The  
387 reason can only partially be attributed to the different drug concentration (5 vs 3 mg/ml), since all  
388 the formulations are at the saturation level and the thermodynamic activity is comparable in all  
389 cases. The TPGS concentration in the formulation (20 vs 10 mM) can contribute to partially explain  
390 the result, since TPGS has widely demonstrated its permeation enhancing capacity resulting from  
391 efflux pumps inhibition and also from the ability to interpose between the phospholipidic bilayers  
392 of cellular membranes modifying their fluidity [33, 49]. To shed light on micelles permeation  
393 mechanisms, we also quantified the amount of TPGS in the cornea. The accumulation of TPGS in the

394 absence of Solutol® (T and TL) gave high and comparable results, even if showing it presents high  
395 variability. The presence of Solutol® markedly decreased TPGS uptake, partially due to the lower  
396 concentration (10 vs 20 mM) and potentially also to a lower mobility of TPGS in the presence of  
397 mixed micelles, as previously demonstrated in the presence of poloxamers [46].  
398 Since the TPGS:cyclosporine weight ratio in the T micelles is approximately 6:1, the data of corneal  
399 retention suggest that the micelles do not penetrate intact in the tissue; the drug is probably  
400 released as the micelles come in contact with the epithelial cells. There are however other  
401 phenomena to be considered, since TPGS could be metabolised in the tissue (see par 3.3).

402  
403 Concerning the relevance of the corneal concentration obtained, we can compare our data with the  
404 ones previously obtained with the commercial formulation Ikervis®, a cationic nanoemulsion  
405 accumulating a cyclosporine amount of  $0.60 \pm 0.14 \mu\text{g}/\text{cm}^2$  [30]. Considering the lower  
406 concentration of cyclosporin in Ikervis® (1 mg/ml), its performance is comparable with TL and ST,  
407 while formulation T markedly enhanced drug uptake. This can be relevant, considering the growing  
408 use of cyclosporine for diseases other than DES [50], that could require higher tissue concentration.

409

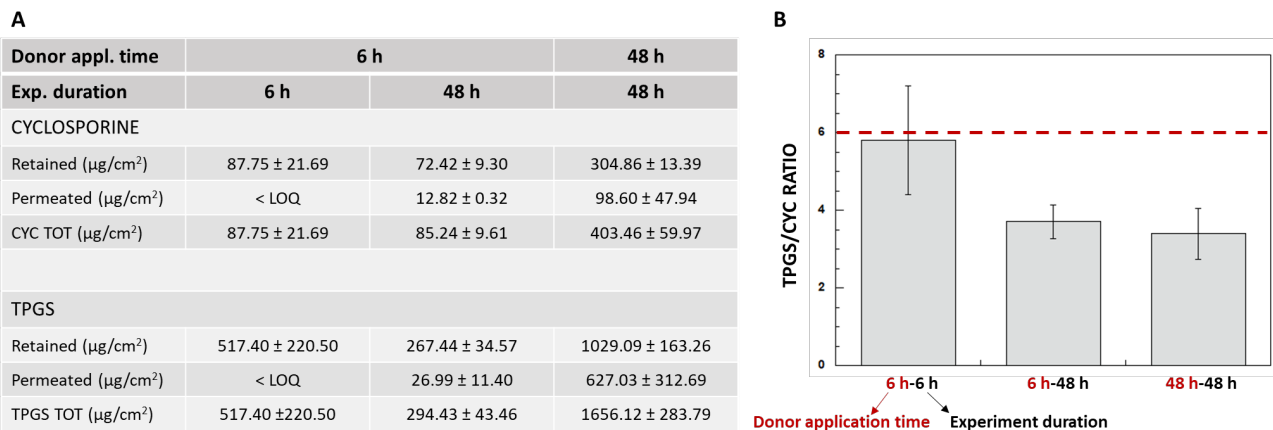
### 410 **3.2.2. Cyclosporine and TPGS diffusion across the sclera from micellar formulations**

411

412 In the last years, the topical route has been proposed for the administration of therapeutics also to  
413 the posterior segment of the eye. This topic is still under investigation: some researchers have  
414 actually highlighted the presence of the drug in the retina, but the clinical significance of the  
415 concentrations found is still subject of debate. The first barrier encountered by the formulation after  
416 topical application is the conjunctiva, which plays a crucial role as it mediates the delivery to the  
417 posterior segment (conjunctival–scleral route), but also the nonproductive and undesirable  
418 systemic absorption. Cyclosporine permeation across the conjunctiva from TPGS micelles was  
419 studied in a previous work [46]. The results highlighted the capability of both drug and TPGS to cross  
420 the conjunctival epithelium in significant amount. However, it is worth mentioning that the fast  
421 nasolacrimal clearance from the conjunctival sac as well as the systemic uptake mediated by blood  
422 and lymphatic vessels reduce the residence time on the eye surface to few minutes, making the  
423 achievement of therapeutic concentrations in the posterior segment unlikely. A possible alternative is  
424 a subconjunctival administration, where the formulation is applied on the surface of the sclera.  
425 Although this procedure cannot be defined non-invasive, it avoids the most serious side effects  
426 connected with the intravitreal injection and, in the presence of a controlled-release formulation,  
427 can reduce the administration frequency. Also in this case, several static, dynamic and metabolic  
428 barriers strongly reduce drug absorption [51], therefore, in order to achieve therapeutic  
429 concentrations at the posterior chamber segment, topical formulations with high concentration of  
430 the drug are required.

431 T micelles, having the higher cyclosporine concentration among the formulations prepared, were  
432 selected for further studies regarding scleral accumulation and permeation. The donor was applied  
433 for 6 h or 48 h and, at the end of the experiment, both the drug and TPGS were quantified in the  
434 receptor phase and inside the scleral tissue. In order to investigate the “reservoir effect” of the  
435 scleral tissue (i.e. the capability to accumulate the drug and then slowly release it to the deeper

436 tissues), the donor was also applied for 6 hours, then removed and the experiment was continued  
 437 up to 48 h. Results of drug and TPGS accumulation and permeation are listed in Figure 2.  
 438 The amount of cyclosporine recovered in the sclera after the 6 h treatment was much higher than  
 439 in the cornea ( $87.75 \pm 21.69 \mu\text{g}/\text{cm}^2$  vs.  $19.81 \pm 4.49 \mu\text{g}/\text{cm}^2$ ), in agreement with the different tissue  
 440 structure, with the sclera being a permeable connective tissue made of collagen fibres. However,  
 441 also in this case, no drug was detected in the receptor phase after 6 h from donor deposition.  
 442 Cyclosporine accumulation increases over time, from  $87.75 \pm 21.69 \mu\text{g}/\text{cm}^2$  after 6 h of contact to  
 443  $304.86 \pm 13.39 \mu\text{g}/\text{cm}^2$  after 48 h of contact. In this last case, it was also detected in the receptor  
 444 compartment, in a very significant amount. When the donor was applied for 6 h and then removed,  
 445 the total amount recovered after 48 h was very similar with respect to the 6 h experiment, but with  
 446 a different distribution: while after 6 h the 100% of the drug was localized in the sclera, after 48 h  
 447 the 15% permeated the tissue, demonstrating the capability of the sclera to slowly release the drug  
 448 and/or the micelles into the deeper tissues.  
 449 The fate of TPGS was also followed. The amount recovered in the sclera after 6 h was approximately  
 450  $500 \mu\text{g}/\text{cm}^2$ . Interestingly, when the donor was applied for 6 h and the quantification was made  
 451 after 48 h, the amount of TPGS decreased to approximately  $300 \mu\text{g}/\text{cm}^2$ . This reduction can be  
 452 attributed to an esterase-mediated hydrolyzation of TPGS with consequent release of vitamin E [30]  
 453 and will be further studied.  
 454



455 Figure 2. Panel A shows the amount of cyclosporine and TPGS accumulated in the sclera and permeated across the  
 456 sclera (average  $\pm$  SD) after formulation application in infinite dose conditions for 6 h and 48 h. The reservoir effect was  
 457 also evaluated by removing the donor after 6 h and continuing the experiment for up to 48 h. Panel B represents  
 458 TPGS/CYC ratio related to the amount accumulated inside the sclera following different donor application times and  
 459 experiment durations. The red line shows the TPGS/cyclosporine ratio (TPGS/CYC) in the T formulation.  
 460

461  
 462 The quantification of TPGS gives the possibility of investigating the mechanisms of micelles  
 463 penetration. The ratio between TPGS (30 mg/ml) and cyclosporine (5 mg/ml) in T micelles is  
 464 approximately 6 (dotted line in Figure 2B). We have then considered drug and TPGS recovered  
 465 (accumulated + permeated) at the end of each experiment and calculated this ratio. The result,  
 466 presented in Figure 2, panel B, shows that the TPGS/cyclosporine ratio of the formulation is  
 467 maintained in case of 6 h experiment duration suggesting that both the polymer and the drug are  
 468 permeated together in form of intact micelles. This is reasonable, if considering the small size of this  
 469 nanocarriers and the relatively high porosity of the sclera. The reduced polymer/drug ratio

470 registered for the other experimental conditions can be attributed to TPGS hydrolysis taking place  
471 in the scleral tissue and particularly evident at long contact times (see par 3.3).

472

473

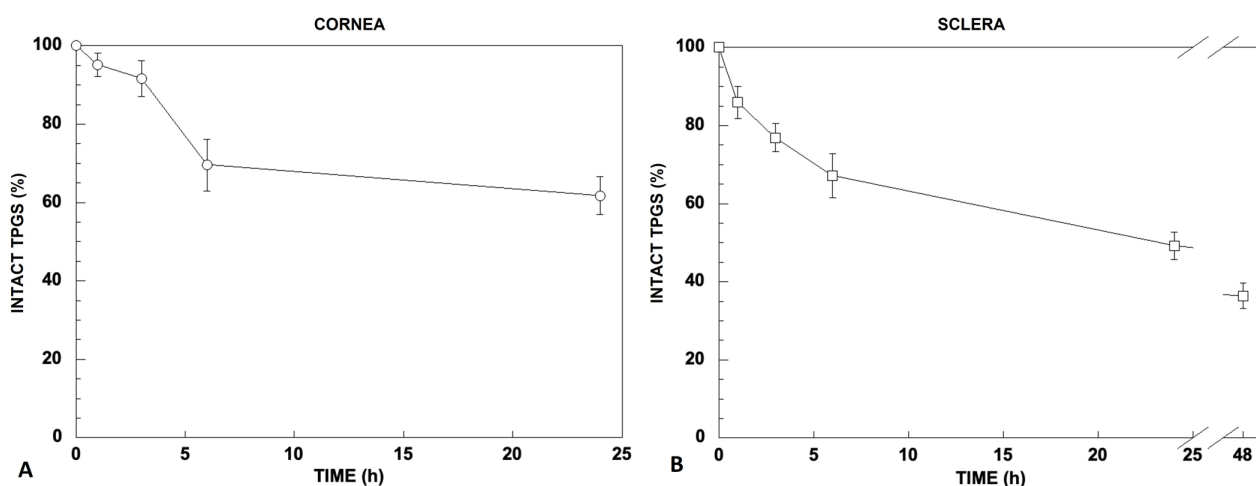
### 474 3.3. TPGS metabolism in contact with ocular tissues

475

476 Previous studies [30, 52] indicate that TPGS, which is stable in solution between pH 4.5 and 7.5, can  
477 be hydrolyzed to vitamin E and vitamin E succinate in the presence of esterases, enzymes  
478 ubiquitously present in tissues and also in the porcine [54] and human [53, 55] cornea and sclera.  
479 However, at the best of our knowledge, the hydrolysis of TPGS in contact with ocular tissues has  
480 never been studied before. This point is relevant since TPGS degradation could cause a reduction or  
481 even loss of the micelles self-assembling properties promoting drug release.

482

483



484

485

486 Figure 3. TPGS metabolism in contact with ocular tissues. Panel A: % of intact TPGS recovered after contact with the  
487 cornea at 37°C; the ratio between TPGS amount (20 µg) and corneal tissue (approx. 50 mg) was around 0.4 µg/mg of  
488 tissue. The data is the mean value of 12 samples from 6 different eyes. Panel B: % of intact TPGS recovered after contact  
489 with the sclera at 37°C; the ratio between TPGS amount (30 µg) and scleral tissue (approx. 60 mg) was around 0.5 µg/mg  
490 of tissue. The data is the mean value of 12 samples from 4 different eyes.

491

492 Overall the results obtained (Figure 3) show a decrease of TPGS concentration in contact with both  
493 cornea and sclera. Although the initial partition of the polymer in the tissue, we can reasonably  
494 hypothesize that this reduction was due to enzymatic degradation since no TPGS reduction occurred  
495 in absence of tissues (control samples) and the HPLC traces highlighted the appearance of vitamin  
496 E succinate and vitamin E. The peaks of these metabolites however, were not enough high and  
497 resolved to be accurately quantified probably because, differently from the situation where TPGS  
498 metabolism was evaluated in solution in the presence of isolated esterase [30], the formed vitamins  
499 (lipophilic) can remain stacked in the tissue. Together with the time required to TPGS to penetrate  
500 the tissue, the degradation profiles obtained depend on esterase concentration and activity in the  
501 two tissues. The faster metabolism in the sclera, clearly visible in the first 3 hours, is in agreement

502 with literature data on 4-nitrophenyl acetate hydrolysis that highlight a 2-fold faster rate of sclera  
503 for comparison with cornea [54].

504 It is difficult to numerically compare these results with the data obtained in the permeation  
505 experiment, given the different conditions in term of TPGS concentration and TPGS/tissue ratio.  
506 However, the data collected support the presence of a relatively fast metabolism inside ocular  
507 tissue. This could help to explain the data obtained in the transscleral experiment and support  
508 cyclosporine release into the tissue owing to TPGS degradation.

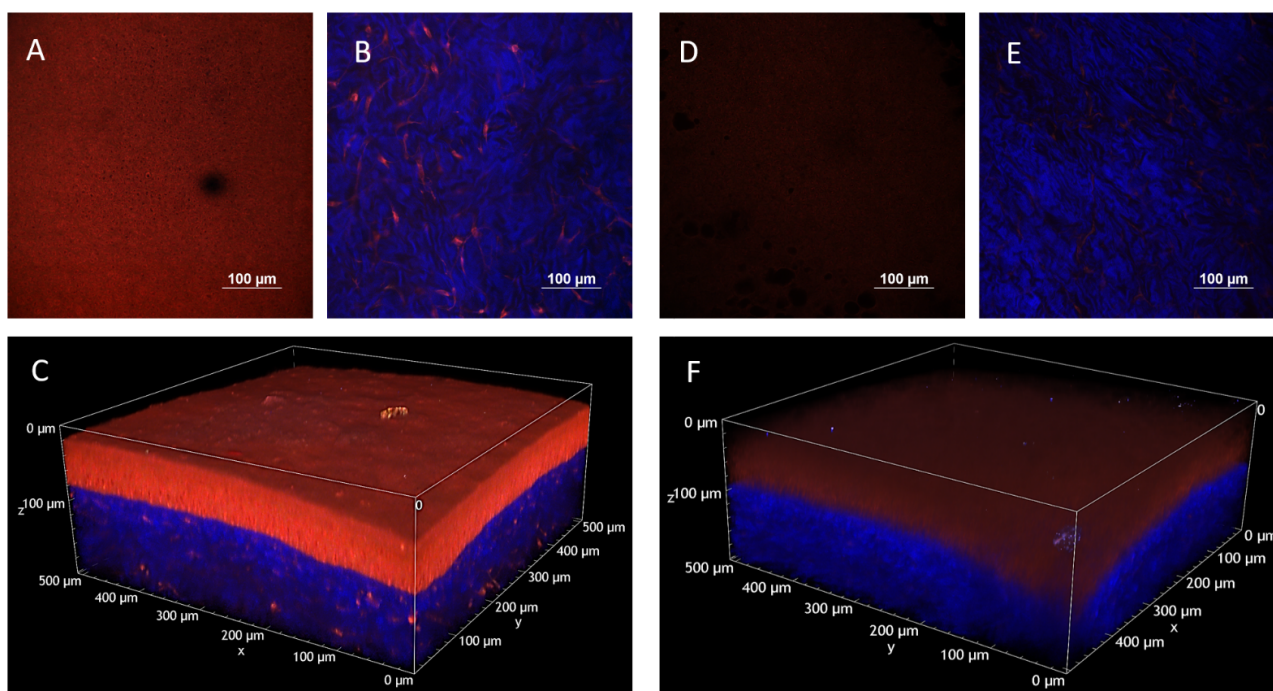
509 It is also worth mentioning that the release of vitamin E and vitamin E succinate, potent antioxidant  
510 compounds, could have a positive effect on the treatment of various ocular diseases, although there  
511 are still conflicting reports on their efficacy [56, 57].

### 513 **3.4 Two-photon microscopy of tissues stained with NR-loaded micelles**

514 To further investigate micelles penetration, Nile Red (NR)-loaded TPGS micelles were prepared;  
515 their size resulted comparable with the blank micelles. Cornea and sclera were treated for 2 hours  
516 with the NR-loaded micelles and the tissues were then imaged with two-photon microscopy with  
517 an irradiation wavelength of 860 or 1080 nm. As reference, a saturated aqueous solution of NR was  
518 used. NR was selected due to the very poor water-solubility (as cyclosporine); additionally, its  
519 emission spectrum is sensitive to the environment polarity [58]. NR, despite being a lipophilic probe,  
520 has notable differences in structure and MW if compared to cyclosporine. This means that we  
521 cannot claim that the behavior of NR-loaded micelles will be exactly the same as the drug-loaded  
522 micelles. However, the data obtained with NR can contribute to understand the behavior of  
523 micelles, when combined with the results obtained using all other techniques.

#### 525 **3.4.1. Two-photon microscopy of corneal tissue stained with NR-loaded micelles**

527 Two-photon microscopy is an advanced technique, allowing for in-depth 3D visualization of  
528 biological tissues without sample handling (*i.e.* fixation, processing, sectioning, staining). In fact, the  
529 specimen is simply fit into a sample holder, moistened with saline solution to avoid dehydration,  
530 and immediately observed. In addition, in comparison to conventional fluorescence or confocal  
531 microscopy, two-photon microscopy uses less energetic photons (in the red and near-infrared  
532 region) thus reducing the photodamage that is instead typically caused by UV and visible light.  
533 Finally, specific asymmetric structures (*e.g.* collagen fibers) can be selectively imaged exploiting the  
534 process of second-harmonic generation [59]. Figure 4 collects the images of the corneal epithelium  
535 and the upper stroma after 2 hours treatment with NR-loaded micelles and with a reference NR  
536 aqueous solution, when excited at 860 nm. In these conditions, NR is mainly detected in the red  
537 channel, while the corneal epithelium gives an autofluorescence signal which falls primarily in the  
538 green spectral region. The stroma is blue, due to the second harmonic generation signal (that falls  
539 at 430 nm at this excitation wavelength) typical of collagen fibers [60], while the presence of  
540 fibroblasts is clearly marked by NR accumulation.



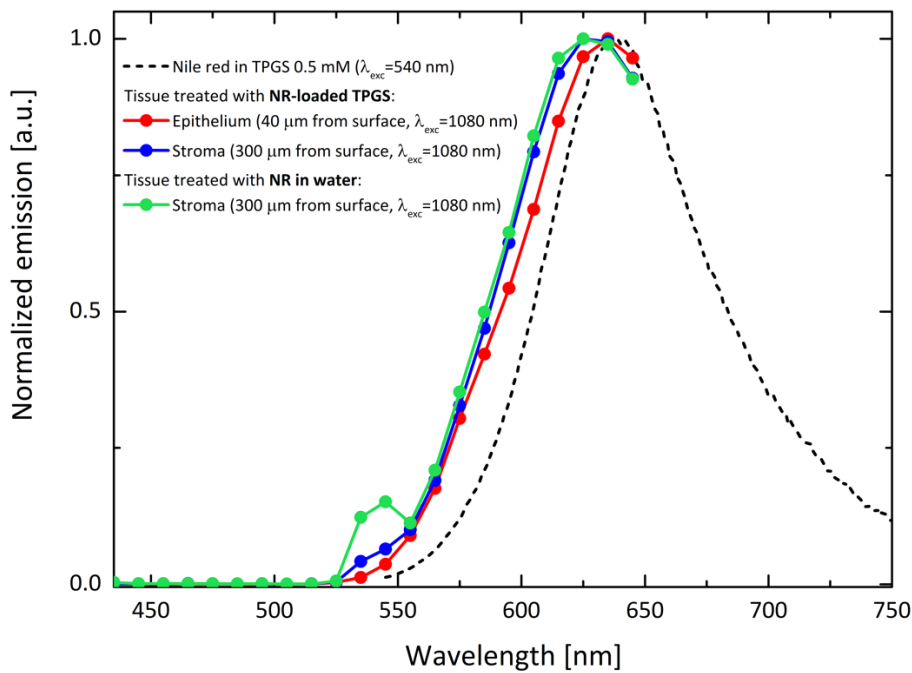
542  
 543 Figure 4. Volume renderings of corneal tissue (epithelium side) reconstructed from Z-stack, acquired with an excitation  
 544 wavelength of 860 nm (SHG from collagen in blue, NR fluorescence detected in both red and green channels). Panel A-  
 545 C: sample treated with TPGS micelles loaded with NR (Z-step: 1  $\mu\text{m}$ , total depth: 202  $\mu\text{m}$ ). Panels A and B: XY scans  
 546 collected at 40 and 300  $\mu\text{m}$  depth, respectively; panel C: 3D overview; Panel D-F: reference treated with NR saturated  
 547 aqueous solution (Z-step: 1  $\mu\text{m}$ , total depth: 202  $\mu\text{m}$ ). Panels D and E: XY scans collected at 40 and 300  $\mu\text{m}$  depth,  
 548 respectively, panel F: 3D overview. All the images in the two Z-scans were acquired with the same detector gains and  
 549 laser power.

550 The intensity of NR signal obtained with the micelles is much higher compared to the reference  
 551 solution, due to the higher fluorescent probe concentration. Similar results were obtained when  
 552 imaging the endothelial side of the tissues (Figure S3).

553 In order to obtain information on micelles-tissue interaction, we acquired emission spectra from  
 554 the tissue at specific focal planes. In fact, being NR a solvatochromic probe [58], the position of its  
 555 emission spectrum changes with the polarity of the environment. This permits to differentiate  
 556 between NR included in the micellar core and NR released and consequently located in cells and/or  
 557 in the intercellular matrix. Spectra were collected exciting the sample at 1080 nm, in order to  
 558 minimize the tissue autofluorescence and maximize at the same time the NR signal.

559 In Figure 5, the emission spectrum of NR in TPGS micelles (black dashed line) is compared with the  
 560 one collected from a corneal sample treated with micelles at a depth of 40  $\mu\text{m}$  (i.e. in the epithelium,  
 561 corresponding to the image in Figure 4A) and 300  $\mu\text{m}$  (i.e. in the corneal stroma, corresponding to  
 562 the image Figure 4B) from the corneal surface. The emission spectrum collected from the tissue is  
 563 shifted toward shorter wavelengths, and the shift increases with increasing depth. The observed  
 564 shift suggests that the probe is located in an environment having a different polarity with respect  
 565 to the micelles, indicating NR release from the nanocarrier. This conclusion is further supported by  
 566 the spectrum obtained from the tissue treated with a NR aqueous solution (green line), which is  
 567 superimposable with the spectrum obtained from the tissue treated with micelles (Figure 5 and  
 568 supplementary material Figure S4), confirming that NR is released from the nanocarrier.

569

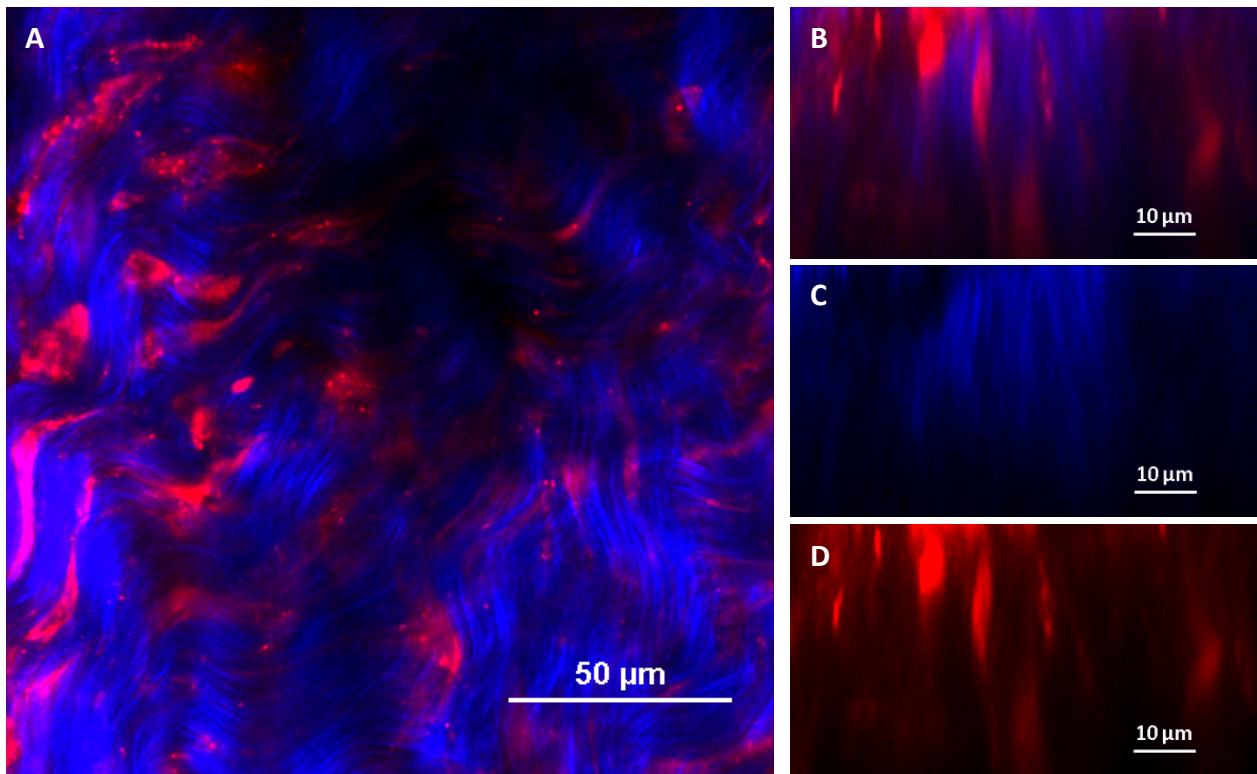


570  
 571 Figure 5. Comparison of the emission spectra recorded in the tissue in correspondence of the epithelium (40  $\mu\text{m}$  from  
 572 surface, red line) and the stroma (300  $\mu\text{m}$  from surface, NR-loaded TPGS: blue line, NR in water: green line) with the  
 573 emission profile of an aqueous solution of NR-loaded TPGS micelles recorded with a fluorometer (black dashed line).

574 The results indicate micelles disassembling in contact with the cornea, in agreement with the data  
 575 of TPGS and cyclosporine corneal retention discussed in par. 3.2.1.

576  
 577 **3.4.2. Two-photon microscopy of scleral tissue stained with NR-loaded micelles**

578  
 579 Figure 6 reports images obtained from a scleral sample treated for 2 hours with NR-loaded micelles,  
 580 upon irradiation at 860 nm. Collagen fibers appear in blue as a result of their second harmonic  
 581 generation (SHG) signal [61], while the red signal is given by NR fluorescence.  
 582



583

584

585

586

587

588

589

590

591

592

593

594

595

596

597

598

599

600

601

602

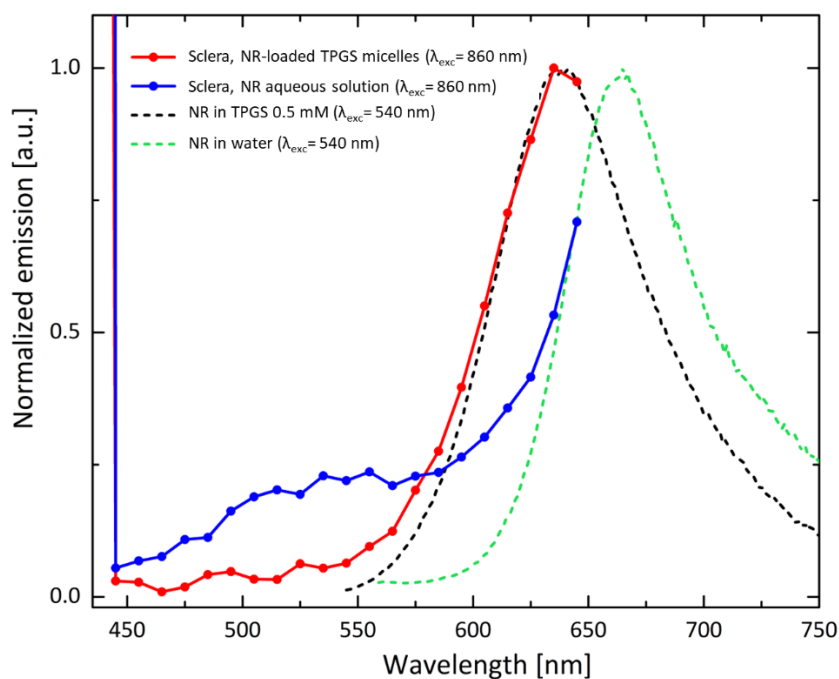
603

604

Figure 6. Panel A represents the scleral structure (XY plane) after treatment with NR-loaded micelles when irradiated at 860 nm (SHG from collagen in blue, NR fluorescence in red). Panel B (blue and red channels overlay), C (blue channel) and D (red channel) represent XZ views of scleral collagen fibers extracted from a Z-stack (image size: 77  $\mu\text{m}$  x 39  $\mu\text{m}$ , Z step: 0.42  $\mu\text{m}$ ).

As shown in figure 6 panel B, C and D, there is no overlap between the blue and red signals, demonstrating that the fluorescent dye arranges in the interfibrillar spaces. Images were collected also upon excitation at 1080 nm and again the signals of collagen fibers and NR were complementary (Figure S5 in the supplementary materials).

As previously described for the cornea, to get further insight into micelles penetration mechanism, emission spectra were recorded from the tissue. First of all, differently from the cornea, the emission profile recorded from the scleral tissue after micelles application is superimposable with the emission spectrum of micelles in solution (see Figure 7), indicating that the probe has not been released and micelles diffuse in their intact form inside the scleral pore. Indeed, the interaction with a cellular tissue such as the cornea affects micelles integrity much more than a collagen-based structure such as the sclera. When the aqueous NR solution was applied to the sclera, the spectrum obtained was clearly shifted toward higher wavelengths (Figure 7), indicating a more hydrophilic environment, in agreement with the presence of hydrated glycosaminoglycans in the interfibrillar spaces. Indeed, the profile is very similar to the one obtained with a spectrofluorometer from an aqueous solution of the dye.



605  
606  
607  
608  
609

Figure 7: Emission spectrum (excitation at 860 nm) recorded in the sclera (100  $\mu$ m from surface) after treatment with NR-loaded TPGS micelles (red line) or the NR saturated aqueous solution (blue line); emission spectrum of NR-loaded TPGS micelles (black dashed line) and NR in water (green dashed line). The last two emission spectra have been acquired using a fluorimeter.

610 Apparently, micelles diffuse intact across the hydrated interfibrillar matrix, and this observation is  
611 in agreement with the quantification of cyclosporine and TPGS inside the sclera, which highlights  
612 that the TPGS/CYC ratio found in the tissue after 6 h of contact corresponds to the one present in  
613 the micellar formulation (Figure 2B).

614 Micelles diffusion occurs in the interfibrillar matrix made of negatively charged hydrated  
615 proteoglycans consisting of a protein core with glycosaminoglycan (GAG) sidechains of repeating  
616 disaccharide units (chondroitin, dermatan, keratan or heparin sulfate) [62, 63]. Indeed, previous  
617 data have demonstrated the ability of TPGS micelles loaded with NR to diffuse intact through a  
618 hyaluronic acid gel [27], possibly due to the presence of the pegylated corona [64]. The inner part  
619 of the sclera is made up of thinner and more regularly arranged collagen fibers that give rise to a  
620 more compact structure [65, 66]. This compact structure, together with the tortuosity of the pores  
621 [67], makes it difficult for the micelles to quickly diffuse into the deepest sclera as evidenced by the  
622 absence of transscleral penetration of cyclosporine after 6 hours of application; micelles can be  
623 slowed down or even get stuck in the sinuous and convoluted pores. However, interaction with the  
624 fibers and/or interfibrillar material together with the enzymatic hydrolysis of the TPGS, determines,  
625 over a longer time, the release of cyclosporine and its delivery to the underlying tissues.

626  
627

### 628 3.3. Study of the effect of TPGS on cornea permeability: transcorneal permeation of 629 fluorescein

630

631 Corneal retentions studies (par 3.2.1) demonstrated the permeation enhancing ability of TPGS. It is  
632 however well known that penetration enhancers can also have irritative effects on the epithelium  
633 and that an important requisite is linked to the possibility to quickly restore tissue barrier properties.

634 In this paper, we used the transcorneal flux of a probe, sodium fluorescein, to assess possible  
635 changes in the tissue permeability determined by TPGS application. Specifically, the cornea was pre-  
636 treated with TPGS 20 mM (i.e. 3% p/v) for 10 minutes, the solution was then removed, the tissue  
637 was rinsed and the permeability of sodium fluorescein was measured. As negative control, a pre-  
638 treatment of 10 minutes with HEPES buffer was used. As positive control, a concentrated (0.1% p/v)  
639 benzalkonium chloride solution was applied.

640 The permeability coefficients obtained are reported in Table 4. The pre-treatment with HEPES buffer  
641 gave a fluorescein permeability coefficient comparable with the previously published data ( $5.00 \pm$   
642  $4.29 \times 10^{-7}$  cm/s) [31], while the use of a concentrated benzalkonium chloride solution  
643 demonstrated to induce a substantial increase in corneal permeability even after only 5 minutes  
644 application, in agreement with literature data [68]. TPGS 20 mM gave a permeability coefficient not  
645 statistically different from the control, confirming a reversible effect at least after 10 minutes  
646 application.

647  
648 Table 4. Permeability coefficient ( $\times 10^{-7}$ ) cm/s of fluorescein sodium across the sclera after pre-treatment with various  
649 excipients.

PRE-TREATMENT	Permeability coefficient ( $\times 10^{-7}$ ) cm/s
HEPES buffer, 10 min	$5.01 \pm 3.32$
TPGS 20 mM (3%), 10 min	$9.83 \pm 5.05$
Benzalkonium chloride 0.1%, 5 min <sup>a</sup>	$28.72 \pm 1.65^{**}$
Benzalkonium chloride 0.1%, 10 min <sup>a</sup>	$55.5 \pm 2.07^{**}$

650 <sup>a</sup>n=2, \*\*statistically different from the HEPES buffer (p<0.001)

651  
652 This application time was selected to better mimic the *in-vivo* conditions characterized by a limited  
653 formulation-tissue contact time. Despite the promising result, the evaluation of the irritation  
654 potential is quite complex and can only be performed *in vivo* and after chronic application. There is  
655 however some encouraging evidence on the good tolerability of this polymer, given by the  
656 commercialization of medical devices containing this compound (Ribocross®; Coqun®) even if at  
657 lower concentration.

### 658 659 **3. Conclusion**

660 The combination of permeation/retention data, hydrolysis results, and two-photon microscopy  
661 images demonstrated the different interaction between nanomicelles and the two different tissues.  
662 Upon contact with the cornea, micelles disassemble and cyclosporin is probably uptaken as a free  
663 molecule. On the contrary, they can penetrate intact into the sclera, at least in the outermost part  
664 of the tissue, characterized by larger collagen fibers, organized in rather irregular bundles. The  
665 interaction of the micelles with the fibers and with the interfibrillar material together with the  
666 enzymatic hydrolysis of the TPGS, determines, in a longer time, the release of cyclosporine and its  
667 transscleral diffusion. The transscleral transport of intact micelles to the choroidal side cannot be  
668 demonstrated by our data, even if it cannot be completely excluded.

669 Overall, TPGS micelles are a very interesting vehicle for cyclosporin ocular delivery, since they are a  
670 water-based formulation with very low irritation potential. They efficiently promote drug  
671 permeation and retention within cornea and sclera and, in the last case, can form a drug reservoir

672 into the tissue that can sustain drug release into deeper tissues for an extended time. This, together  
673 with the relatively high drug concentration, could reduce administration frequency thus increasing  
674 patient's compliance. Additionally, TPGS hydrolysis determines vitamin E and vitamin E succinate  
675 release, with an antioxidant activity that can potentially contribute to the improvement of  
676 oxidation-mediated diseases. Finally, it is worth mentioning the easy preparation procedure, the  
677 possibility of sterilization by filtration and the good stability.

678  
679  
680

#### 681 **Authors contributions**

682 Martina Ghezzi: conceptualization, methodology, investigation, writing-original draft preparation,  
683 writing - review and editing; Ilaria Ferraboschi: investigation, writing – review and editing; Andrea  
684 Delledonne: methodology, investigation, writing – review and editing; Silvia Pescina: methodology,  
685 validation, writing – review and editing; Cristina Padula: validation, writing – review and editing;  
686 Patrizia Santi: writing – review and editing, funding acquisition; Cristina Sissa: validation, writing –  
687 review and editing, funding acquisition; Francesca Terenziani: methodology, writing – review and  
688 editing, funding acquisition; Sara Nicoli: conceptualization, methodology, writing - original draft  
689 preparation, writing - review and editing, funding acquisition. All authors have read and agreed to  
690 the published version of the manuscript.

691  
692

#### 693 **Funding**

694 This work was supported by a Grant from the Italian Ministry of Research (Grant PRIN 2017 #  
695 20173ZECCM Tackling biological barriers to antigen delivery by nanotechnological vaccines  
696 (NanoTechVax). Andrea Delledonne, Ilaria Ferraboschi, Cristina Sissa and Francesca Terenziani  
697 benefited from the equipment and support of the COMP-HUB Initiative, funded by the  
698 “Departments of Excellence” program of the Italian Ministry for Education, University and Research  
699 (MIUR, 2018–2022). We acknowledge the financial support of the University of Parma (Bando di  
700 accesso al Fondo Attrezzature Scientifiche 2018), for the purchase of the two-photon microscopy  
701 facility. Ilaria Ferraboschi benefited of a PhD fellowship financed by PON R&I 2014-2020 (FSE REACT-  
702 EU fundings). This work has received funding from the European Union's Horizon 2020 research and  
703 innovation programme under the Marie Skłodowska-Curie grant agreement No 101007804  
704 (Micro4Nano).

705

#### 706 **Acknowledgments**

707 Authors gratefully thank Pierugo Cavallini and Macello Annoni SpA for kindly providing porcine eye  
708 bulbs. Former undergraduate students Daisy Sorgi, Alessia Filippini and Francesca Di Pancrazio are  
709 gratefully acknowledged for their contribution in data collection.

710

#### 711 **Declaration of competing interest**

712 The authors declare that they have no known competing financial interests or personal relationships  
713 that could have appeared to influence the work reported in this paper.

714

715 **Disclosures**

716 Partially presented (poster) at PBP World Meeting 2022, Rotterdam, 28-31 March 2022: “Micelles-  
717 loaded polymeric films to improve cyclosporine solubility and ocular delivery to the posterior  
718 segment”, M. Ghezzi, S. Pescina, C. Padula, P. Santi, S. Nicoli.

719

720 **References:**

721 [1] M. Krönke, W.J. Leonard, J.M. Depper, S.K. Arya, F. Wong-Staal, R.C. Gallo, T.A. Waldmann, W.C.  
722 Greene, Cyclosporin A inhibits T-cell growth factor gene expression at the level of mRNA  
723 transcription, *Proceedings of the National Academy of Sciences*, 81 (1984) 5214.

724 [2] V. Gupta, P.K. Sahu, Topical cyclosporin A in the management of vernal keratoconjunctivitis, *Eye*,  
725 15 (2001) 39-41.

726 [3] S. Tatlipinar, E.K. Akpek, Topical ciclosporin in the treatment of ocular surface disorders, *The*  
727 *British journal of ophthalmology*, 89 (2005) 1363-1367.

728 [4] S.N. Rao, Comparison of the Efficacy of Topical Cyclosporine 0.05% Compared With Tobradex for  
729 the Treatment of Posterior Blepharitis, *Investigative Ophthalmology & Visual Science*, 46 (2005)  
730 2662-2662.

731 [5] M. Rubin, S.N. Rao, Efficacy of Topical Cyclosporin 0.05% in the Treatment of Posterior  
732 Blepharitis, *Journal of Ocular Pharmacology and Therapeutics*, 22 (2006) 47-53.

733 [6] A.T. Vitale, A. Rodriguez, C.S. Foster, Low-dose Cyclosporin A Therapy in Treating Chronic,  
734 Noninfectious Uveitis, *Ophthalmology*, 103 (1996) 365-374.

735 [7] R.J. Barry, Q.D. Nguyen, R.W. Lee, P.I. Murray, A.K. Denniston, Pharmacotherapy for uveitis:  
736 current management and emerging therapy, *Clinical ophthalmology (Auckland, N.Z.)*, 8 (2014) 1891-  
737 1911.

738 [8] Z. Saleh, T. Arayssi, Update on the therapy of Behçet disease, *Therapeutic Advances in Chronic*  
739 *Disease*, 5 (2014) 112-134.

740 [9] F. Lallemand, O. Felt-Baeyens, K. Besseghir, F. Behar-Cohen, R. Gurny, Cyclosporine A delivery to  
741 the eye: A pharmaceutical challenge, *European Journal of Pharmaceutics and Biopharmaceutics*, 56  
742 (2003) 307-318.

743 [10] N. El Tayar, A.E. Mark, P. Vallat, R.M. Brunne, B. Testa, W.F. van Gunsteren, Solvent-dependent  
744 conformation and hydrogen-bonding capacity of cyclosporin A: evidence from partition coefficients  
745 and molecular dynamics simulations, *Journal of Medicinal Chemistry*, 36 (1993) 3757-3764.

746 [11] F. Lallemand, M. Schmitt, J.-L. Bourges, R. Gurny, S. Benita, J.-S. Garrigue, Cyclosporine A  
747 delivery to the eye: A comprehensive review of academic and industrial efforts, *European Journal*  
748 *of Pharmaceutics and Biopharmaceutics*, 117 (2017) 14-28.

749 [12] A. Patel, K. Cholkar, V. Agrahari, A.K. Mitra, Ocular drug delivery systems: An overview, *World*  
750 *journal of pharmacology*, 2 (2013) 47-64.

751 [13] M. Ghezzi, S. Pescina, C. Padula, P. Santi, E. Del Favero, L. Cantù, S. Nicoli, Polymeric micelles in  
752 drug delivery: An insight of the techniques for their characterization and assessment in biorelevant  
753 conditions, *Journal of Controlled Release*, 332 (2021) 312-336.

754 [14] Polymeric micelles for ocular drug delivery: From structural frameworks to recent preclinical  
755 studies, *Journal of Controlled Release*, 248 (2017) 96 - 116.

756 [15] M.A. Toscanini, M.J. Limeres, A.V. Garrido, M. Cagel, E. Bernabeu, M.A. Moretton, D.A.  
757 Chiappetta, M.L. Cuestas, Polymeric micelles and nanomedicines: Shaping the future of next  
758 generation therapeutic strategies for infectious diseases, *Journal of Drug Delivery Science and*  
759 *Technology*, 66 (2021) 102927.

760 [16] M.A. Grimaudo, S. Pescina, C. Padula, P. Santi, A. Concheiro, C. Alvarez-Lorenzo, S. Nicoli,  
761 Topical application of polymeric nanomicelles in ophthalmology: a review on research efforts for  
762 the noninvasive delivery of ocular therapeutics, *Expert Opinion on Drug Delivery*, 16 (2019) 397-  
763 413.

764 [17] Y. Yu, D. Chen, Y. Li, W. Yang, J. Tu, Y. Shen, Improving the topical ocular pharmacokinetics of  
765 lyophilized cyclosporine A-loaded micelles: formulation, in vitro and in vivo studies, *Drug delivery*,  
766 25 (2018) 888-899.

767 [18] A. Varela-Garcia, A. Concheiro, C. Alvarez-Lorenzo, Soluplus micelles for acyclovir ocular  
768 delivery: Formulation and cornea and sclera permeability, *International Journal of Pharmaceutics*,  
769 552 (2018) 39-47.

770 [19] Z. Li, M. Liu, L. Ke, L.-J. Wang, C. Wu, C. Li, Z. Li, Y.-L. Wu, Flexible polymeric nanosized micelles  
771 for ophthalmic drug delivery: research progress in the last three years, *Nanoscale Advances*, 3  
772 (2021) 5240-5254.

773 [20] C. Di Tommaso, J.-L. Bourges, F. Valamanesh, G. Trubitsyn, A. Torriglia, J.-C. Jeanny, F. Behar-  
774 Cohen, R. Gurny, M. Möller, Novel micelle carriers for cyclosporin A topical ocular delivery: In vivo  
775 cornea penetration, ocular distribution and efficacy studies, *European Journal of Pharmaceutics and*  
776 *Biopharmaceutics*, 81 (2012) 257-264.

777 [21] R.D. Vaishya, M. Gokulgandhi, S. Patel, M. Minocha, A.K. Mitra, Novel Dexamethasone-Loaded  
778 Nanomicelles for the Intermediate and Posterior Segment Uveitis, *AAPS PharmSciTech*, 15 (2014)  
779 1238-1251.

780 [22] N. Elsaid, S. Somavarapu, T.L. Jackson, Cholesterol-poly(ethylene) glycol nanocarriers for the  
781 transscleral delivery of sirolimus, *Experimental Eye Research*, 121 (2014) 121-129.

782 [23] C. Peng, L. Kuang, J. Zhao, A.E. Ross, Z. Wang, J.B. Ciolino, Bibliometric and visualized analysis  
783 of ocular drug delivery from 2001 to 2020, *Journal of Controlled Release*, 345 (2022) 625-645.

784 [24] Polymeric micelles in mucosal drug delivery: Challenges towards clinical translation,  
785 *Biotechnology Advances*, 33 (2015) 1380 - 1392.

786 [25] Y. Wang, L. Jiang, Q. Shen, J. Shen, Y. Han, H. Zhang, Investigation on the self-assembled  
787 behaviors of C18 unsaturated fatty acids in arginine aqueous solution, *RSC Advances*, 7 (2017)  
788 41561-41572.

789 [26] A.-L. Fameau, A. Arnould, A. Saint-Jalmes, Responsive self-assemblies based on fatty acids,  
790 *Current Opinion in Colloid & Interface Science*, 19 (2014) 471-479.

791 [27] M. Ghezzi, S. Pescina, A. Delledonne, I. Ferraboschi, C. Sissa, F. Terenziani, P.D.F.R. Remiro, P.  
792 Santi, S. Nicoli, Improvement of Imiquimod Solubilization and Skin Retention via TPGS Micelles:  
793 Exploiting the Co-Solubilizing Effect of Oleic Acid, *Pharmaceutics*, 13 (2021) 1476.

794 [28] S. Tampucci, L. Guazzelli, S. Burgalassi, S. Carpi, P. Chetoni, A. Mezzetta, P. Nieri, B. Polini, C.S.  
795 Pomelli, E. Terreni, D. Monti, pH-Responsive Nanostructures Based on Surface Active Fatty Acid-  
796 Protic Ionic Liquids for Imiquimod Delivery in Skin Cancer Topical Therapy, *Pharmaceutics*, 12 (2020)  
797 1078.

798 [29] G. Ismailos, C. Reppas, J.B. Dressman, P. Macheras, Unusual solubility behaviour of cyclosporin  
799 A in aqueous media, *Journal of Pharmacy and Pharmacology*, 43 (1991) 287-289.

800 [30] M.A. Grimaudo, S. Pescina, C. Padula, P. Santi, A. Concheiro, C. Alvarez-Lorenzo, S. Nicoli,  
801 Poloxamer 407/TPGS Mixed Micelles as Promising Carriers for Cyclosporine Ocular Delivery, *Mol*  
802 *Pharm*, 15 (2018) 571-584.

803 [31] S. Pescina, P. Govoni, A. Potenza, C. Padula, P. Santi, S. Nicoli, Development of a Convenient ex  
804 vivo Model for the Study of the Transcorneal Permeation of Drugs: Histological and Permeability  
805 Evaluation, *Journal of Pharmaceutical Sciences*, 104 (2015) 63-71.

806 [32] R.D. Bachu, P. Chowdhury, Z.H.F. Al-Saedi, P.K. Karla, S.H.S. Boddu, Ocular Drug Delivery  
807 Barriers—Role of Nanocarriers in the Treatment of Anterior Segment Ocular Diseases,  
808 *Pharmaceutics*, 10 (2018) 28.

809 [33] C. Ostacolo, C. Caruso, D. Tronino, S. Troisi, S. Laneri, L. Pacente, A. Del Prete, A. Sacchi,  
810 Enhancement of corneal permeation of riboflavin-5'-phosphate through vitamin E TPGS: A  
811 promising approach in corneal trans-epithelial cross linking treatment, *International Journal of*  
812 *Pharmaceutics*, 440 (2013) 148-153.

813 [34] M.H. Warsi, M. Anwar, V. Garg, G.K. Jain, S. Talegaonkar, F.J. Ahmad, R.K. Khar, Dorzolamide-  
814 loaded PLGA/vitamin E TPGS nanoparticles for glaucoma therapy: Pharmacoscintigraphy study and  
815 evaluation of extended ocular hypotensive effect in rabbits, *Colloids and Surfaces B: Biointerfaces*,  
816 122 (2014) 423-431.

817 [35] M. Alkholief, H. Albasit, A. Alhowyan, S. Alshehri, M. Raish, M. Abul Kalam, A. Alshamsan,  
818 Employing a PLGA-TPGS based nanoparticle to improve the ocular delivery of Acyclovir, *Saudi*  
819 *Pharmaceutical Journal*, 27 (2019) 293-302.

820 [36] E.-M. Collnot, C. Baldes, M.F. Wempe, R. Kappl, J. Hüttermann, J.A. Hyatt, K.J. Edgar, U.F.  
821 Schaefer, C.-M. Lehr, Mechanism of Inhibition of P-Glycoprotein Mediated Efflux by Vitamin E TPGS:  
822 Influence on ATPase Activity and Membrane Fluidity, *Molecular Pharmaceutics*, 4 (2007) 465-474.

823 [37] A.W.G. Alani, D.A. Rao, R. Seidel, J. Wang, J. Jiao, G.S. Kwon, The Effect of Novel Surfactants and  
824 Solutol® HS 15 on Paclitaxel Aqueous Solubility and Permeability Across a Caco-2 Monolayer, *Journal*  
825 *of Pharmaceutical Sciences*, 99 (2010) 3473-3485.

826 [38] L. Song, Y. Shen, J. Hou, L. Lei, S. Guo, C. Qian, Polymeric micelles for parenteral delivery of  
827 curcumin: Preparation, characterization and in vitro evaluation, *Colloids and Surfaces A:*  
828 *Physicochemical and Engineering Aspects*, 390 (2011) 25-32.

829 [39] N.F. Younes, S.A. Abdel-Halim, A.I. Ellassasy, Solutol HS15 based binary mixed micelles with  
830 penetration enhancers for augmented corneal delivery of sertaconazole nitrate: optimization, in  
831 vitro, ex vivo and in vivo characterization, *Drug Delivery*, 25 (2018) 1706-1717.

832 [40] P.F. Hoyng, N. Verbey, L. Thörig, N.J. van Haeringen, Topical prostaglandins inhibit trauma-  
833 induced inflammation in the rabbit eye, *Investigative Ophthalmology & Visual Science*, 27 (1986)  
834 1217-1225.

835 [41] A. Macrì, S. Giuffrida, V. Amico, M. Iester, C.E. Traverso, Effect of linoleic acid and  $\gamma$ -linolenic  
836 acid on tear production, tear clearance and on the ocular surface after photorefractive keratectomy,  
837 *Graefe's Archive for Clinical and Experimental Ophthalmology*, 241 (2003) 561-566.

838 [42] S. Barabino, M. Rolando, P. Camicione, G. Ravera, S. Zanardi, S. Giuffrida, G. Calabria, Systemic  
839 Linoleic and  $\gamma$ -Linolenic Acid Therapy in Dry Eye Syndrome With an Inflammatory Component,  
840 *Cornea*, 22 (2003).

841 [43] I. Molina-Leyva, A. Molina-Leyva, A. Bueno-Cavanillas, Efficacy of nutritional supplementation  
842 with omega-3 and omega-6 fatty acids in dry eye syndrome: a systematic review of randomized  
843 clinical trials, *Acta Ophthalmologica*, 95 (2017) e677-e685.

844 [44] J.S. Fogt, N. Fogt, P.E. King-Smith, H. Liu, J.T. Barr, Changes in Tear Lipid Layer Thickness and  
845 Symptoms Following the Use of Artificial Tears with and Without Omega-3 Fatty Acids: A  
846 Randomized, Double-Masked, Crossover Study, *Clinical ophthalmology (Auckland, N.Z.)*, 13 (2019)  
847 2553-2561.

848 [45] S. Rashid, Y. Jin, T. Ecoiffier, S. Barabino, D.A. Schaumberg, M.R. Dana, Topical Omega-3 and  
849 Omega-6 Fatty Acids for Treatment of Dry Eye, *Archives of Ophthalmology*, 126 (2008) 219-225.

850 [46] S. Pescina, L.G. Lucca, P. Govoni, C. Padula, E.D. Favero, L. Cantù, P. Santi, S. Nicoli, Ex Vivo  
851 Conjunctival Retention and Transconjunctival Transport of Poorly Soluble Drugs Using Polymeric  
852 Micelles, *Pharmaceutics*, 11 (2019) 476.

853 [47] S. Shubber, D. Vllasaliu, C. Rauch, F. Jordan, L. Illum, S. Stolnik, Mechanism of mucosal  
854 permeability enhancement of CriticalSorb® (Solutol® HS15) investigated in vitro in cell cultures,  
855 *Pharmaceutical research*, 32 (2015) 516-527.

856 [48] I. Pepić, J. Lovrić, J. Filipović-Grčić, How do polymeric micelles cross epithelial barriers?,  
857 *European Journal of Pharmaceutical Sciences*, 50 (2013) 42-55.

858 [49] M.S. Shahab, M. Rizwanullah, S. Sarim Imam, Formulation, optimization and evaluation of  
859 vitamin E TPGS emulsified dorzolamide solid lipid nanoparticles, *Journal of Drug Delivery Science*  
860 *and Technology*, 68 (2022) 103062.

861 [50] A. Labbé, C. Baudouin, D. Ismail, M. Amrane, J.S. Garrigue, A. Leonardi, F.C. Figueiredo, G. Van  
862 Setten, M. Labetoulle, Pan-European survey of the topical ocular use of cyclosporine A, *Journal*  
863 *Français d'Ophtalmologie*, 40 (2017) 187-195.

864 [51] E. Eljarrat-Binstock, J. Pe'er, A.J. Domb, New Techniques for Drug Delivery to the Posterior Eye  
865 Segment, *Pharmaceutical Research*, 27 (2010) 530-543.

866 [52] M.G. Traber, C.A. Thellman, M.J. Rindler, H.J. Kayden, Uptake of intact TPGS (d-alpha-  
867 tocopheryl polyethylene glycol 1000 succinate) a water-miscible form of vitamin E by human cells  
868 in vitro, *The American Journal of Clinical Nutrition*, 48 (1988) 605-611.

869 [53] S. Duvvuri, S. Majumdar, K.A. Mitra, Role of Metabolism in Ocular Drug Delivery, *Current Drug*  
870 *Metabolism*, 5 (2004) 507-515.

871 [54] E.M. Heikkinen, E.M. del Amo, V.-P. Ranta, A. Urtti, K.-S. Vellonen, M. Ruponen, Esterase activity  
872 in porcine and albino rabbit ocular tissues, *European Journal of Pharmaceutical Sciences*, 123 (2018)  
873 106-110.

874 [55] P. Ichhpujani, L.J. Katz, G. Hollo, C.L. Shields, J.A. Shields, B. Marr, R. Eagle, H. Alvim, S.S. Wizov,  
875 A. Acheampong, J. Chen, L.A. Wheeler, Comparison of Human Ocular Distribution of Bimatoprost  
876 and Latanoprost, *Journal of Ocular Pharmacology and Therapeutics*, 28 (2011) 134-145.

877 [56] A.K. Grover, S.E. Samson, Antioxidants and vision health: facts and fiction, *Molecular and*  
878 *Cellular Biochemistry*, 388 (2014) 173-183.

879 [57] M.M. McCusker, K. Durrani, M.J. Payette, J. Suchecki, An eye on nutrition: The role of vitamins,  
880 essential fatty acids, and antioxidants in age-related macular degeneration, dry eye syndrome, and  
881 cataract, *Clinics in Dermatology*, 34 (2016) 276-285.

882 [58] B. Boldrini, E. Cavalli, A. Painelli, F. Terenziani, Polar Dyes in Solution: A Joint Experimental and  
883 Theoretical Study of Absorption and Emission Band Shapes, *The Journal of Physical Chemistry A*, 106  
884 (2002) 6286-6294.

885 [59] F. Helmchen, W. Denk, Deep tissue two-photon microscopy, *Nature Methods*, 2 (2005) 932-  
886 940.

887 [60] C.Y. Park, J.K. Lee, R.S. Chuck, Second Harmonic Generation Imaging Analysis of Collagen  
888 Arrangement in Human Cornea, *Investigative Ophthalmology & Visual Science*, 56 (2015) 5622-  
889 5629.

890 [61] M. Zyablitskaya, E.L. Munteanu, T. Nagasaki, D.C. Paik, Second Harmonic Generation Signals in  
891 Rabbit Sclera As a Tool for Evaluation of Therapeutic Tissue Cross-linking (TXL) for Myopia, *Journal*  
892 *of visualized experiments : JoVE*, (2018) 56385.

893 [62] P.G. Watson, R.D. Young, Scleral structure, organisation and disease. A review, *Experimental*  
894 *Eye Research*, 78 (2004) 609-623.

895 [63] J.G. Hollyfield, M.E. Rayborn, M. Tammi, R. Tammi, Hyaluronan in the Interphotoreceptor  
896 Matrix of the Eye: Species Differences in Content, Distribution, Ligand Binding and degradation,  
897 *Experimental Eye Research*, 66 (1998) 241-248.

898 [64] J. Puig-Rigall, C. Fernández-Rubio, J. González-Benito, J.E. Houston, A. Radulescu, P. Nguewa, G.  
899 González-Gaitano, Structural characterization by scattering and spectroscopic methods and

900 biological evaluation of polymeric micelles of poloxamines and TPGS as nanocarriers for miltefosine  
901 delivery, *International Journal of Pharmaceutics*, 578 (2020) 119057.

902 [65] J.K. Pijanka, B. Coudrillier, K. Ziegler, T. Sorensen, K.M. Meek, T.D. Nguyen, H.A. Quigley, C.  
903 Boote, Quantitative Mapping of Collagen Fiber Orientation in Non-glaucoma and Glaucoma  
904 Posterior Human Sclerae, *Investigative Ophthalmology & Visual Science*, 53 (2012) 5258-5270.

905 [66] Y. Komai, T. Ushiki, The three-dimensional organization of collagen fibrils in the human cornea  
906 and sclera, *Investigative Ophthalmology & Visual Science*, 32 (1991) 2244-2258.

907 [67] K.M. Hämäläinen, K. Kananen, S. Auriola, K. Kontturi, A. Urtti, Characterization of paracellular  
908 and aqueous penetration routes in cornea, conjunctiva, and sclera, *Investigative Ophthalmology &  
909 Visual Science*, 38 (1997) 627-634.

910 [68] W. Chen, Z. Li, J. Hu, Z. Zhang, L. Chen, Y. Chen, Z. Liu, Corneal Alterations Induced by Topical  
911 Application of Benzalkonium Chloride in Rabbit, *PLOS ONE*, 6 (2011) e26103.

912 [69] E. Donnenfeld, S.C. Pflugfelder, Topical Ophthalmic Cyclosporine: Pharmacology and Clinical  
913 Uses, *Survey of Ophthalmology*, 54 (2009) 321-338.

914 [70] G.J. Jaffe, C.-S. Yang, X.-C. Wang, S.W. Cousins, R.P. Gallemore, P. Ashton, Intravitreal sustained-  
915 release cyclosporine in the treatment of experimental uveitis, *Ophthalmology*, 105 (1998) 46-56.

916